



**HAL**  
open science

## Ex vivo skin diffusion and decontamination studies of titanium dioxide nanoparticles

Adeline Tarantini, Emilie Jamet-Anselme, Sabine Lam, Vincent Haute, David Suhard, Nathalie Valle, Véronique Chamel-Mossuz, Céline Bouvier-Capely, Guillaume Phan

### ► To cite this version:

Adeline Tarantini, Emilie Jamet-Anselme, Sabine Lam, Vincent Haute, David Suhard, et al.. Ex vivo skin diffusion and decontamination studies of titanium dioxide nanoparticles. *Toxicology in Vitro*, 2024, 101, pp.105918. 10.1016/j.tiv.2024.105918 . irsn-04693491

**HAL Id: irsn-04693491**

**<https://irsn.hal.science/irsn-04693491v1>**

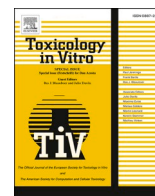
Submitted on 10 Sep 2024

**HAL** is a multi-disciplinary open access archive for the deposit and dissemination of scientific research documents, whether they are published or not. The documents may come from teaching and research institutions in France or abroad, or from public or private research centers.

L'archive ouverte pluridisciplinaire **HAL**, est destinée au dépôt et à la diffusion de documents scientifiques de niveau recherche, publiés ou non, émanant des établissements d'enseignement et de recherche français ou étrangers, des laboratoires publics ou privés.



Distributed under a Creative Commons Attribution - NonCommercial - NoDerivatives 4.0 International License



## Ex vivo skin diffusion and decontamination studies of titanium dioxide nanoparticles

Adeline Tarantini<sup>a</sup>, Emilie Jamet-Anselme<sup>b</sup>, Sabine Lam<sup>c</sup>, Vincent Haute<sup>a</sup>, David Suhard<sup>c</sup>, Nathalie Valle<sup>d</sup>, Véronique Chamel-Mossuz<sup>a</sup>, Céline Bouvier-Capely<sup>c</sup>, Guillaume Phan<sup>c,\*</sup>

<sup>a</sup> Univ. Grenoble Alpes, CEA, Nanosafety Platform (PNS), Laboratory of Medical Biology (LBM), Grenoble, France

<sup>b</sup> Service de Protection Radiologique des Armées, Clamart, France

<sup>c</sup> Institut de Radioprotection et de Sécurité Nucléaire, Laboratoire de Radiochimie, Spéciation et Imagerie, IBISA-Paradis Platform, Fontenay-aux-Roses, France

<sup>d</sup> Luxembourg Institute of Science and Technology, Luxembourg

### ARTICLE INFO

Editor: Maxime Culot

#### Keywords:

Titanium dioxide nanoparticles

Skin diffusion

Ex vivo

Decontamination

Cleansing products

### ABSTRACT

This study aims to adapt an experimental model based on Franz diffusion cells and porcine skin explants to characterize the diffusion of TiO<sub>2</sub> NPs and to compare the efficacy of different cleansing products, soapy water and a calixarene cleansing nanoemulsion compared with pure water, as a function of the time of treatment.

While TiO<sub>2</sub> NPs tend to form agglomerates in aqueous solutions, a diffusion through healthy skin was confirmed as particles were detected in the receptor fluid of Franz cells using sp-ICP-MS. In the absence of treatment, SIMS images showed the accumulation of TiO<sub>2</sub> agglomerates in the stratum corneum, the epidermis, the dermis, and around hair follicles. Decontamination assays showed that the two products tested were comparably effective in limiting Ti penetration, whatever the treatment time. However, only calixarene nanoemulsion was statistically more efficient than water in retaining TiO<sub>2</sub> in the donor compartment (>89%), limiting retention inside the skin (<1%) and preventing NP diffusion through the skin (<0.13%) when treatments were initiated 30 min after skin exposure. When decontamination was delayed from 30 min to 6 h, the amount of Ti diffusing and retained in the skin increased.

This study demonstrates that TiO<sub>2</sub> NPs may diffuse through healthy skin after exposure. Thus, effective decontamination using cleansing products should be carried out as soon as possible.

### 1. Introduction

Since their emergence in the 1980s, nanotechnologies have developed considerably, contributing to numerous technological advances in many fields, including healthcare, agriculture, energy, and chemistry for instance (Malik et al., 2023). One of the consequences has been an increase in the number of workers potentially exposed to engineered nanomaterials (ENMs). The number of workers exposed to ENMs worldwide is not known, but nanotechnologies could affect 6 million researchers and workers in 2020, based on an extrapolation (Roco, 2011). However, despite recent advances in knowledge of the potential adverse effects of exposure to ENMs, risk assessment remains a challenging task due to the wide variety of ENMs and their unique physicochemical properties, which can modulate their fate and toxicity.

Occupational exposure can occur throughout the ENMs life cycle, from manufacture and processing to disposal or recycling (Schulte et al.,

2008). Although inhalation is the main route of exposure to ENMs, skin can be another relevant route of exposure in the workplaces (Bergamaschi, 2009). The skin is the largest organ in the body and comprises three main layers: the epidermis, dermis and hypodermis, which are associated with several appendages such as hair follicles or sweat glands. The epidermis, the outer layer of the skin, contains several strata, namely stratum corneum (SC), stratum lucidum (SL), stratum granulosum (SG), stratum spinosum (SS) and stratum basale (SB), while the dermis and hypodermis are connective tissues containing blood and lymphatic vessels.

The penetration of substances, including nanoparticles (NPs), through the different layers of the skin into the systemic circulation is fairly complex and involves three main phases.

Penetration refers to the entry and diffusion of compounds through the stratum corneum, where they may either accumulate or enter the bloodstream. Permeation is the diffusion of the compound through

\* Corresponding author.

E-mail address: [guillaume.phan@irsn.fr](mailto:guillaume.phan@irsn.fr) (G. Phan).

<https://doi.org/10.1016/j.tiv.2024.105918>

Received 30 April 2024; Received in revised form 23 July 2024; Accepted 11 August 2024

Available online 13 August 2024

0887-2333/© 2024 The Authors. Published by Elsevier Ltd. This is an open access article under the CC BY license (<http://creativecommons.org/licenses/by/4.0/>).

successive deeper layers to the dermis. Finally, resorption is the absorption of the compound into the vascular system. Some studies suggested that NPs can also “mechanically” accumulate in appendages such as hair follicles after application to the skin (Lekki et al., 2007), or penetrate the interstitial spaces of the skin (Bennett et al., 2012).

Existing data on the dermal absorption of NPs are quite conflicting, with some studies showing that NPs can penetrate the SC while others demonstrate that NPs can diffuse through deeper layers to the systemic circulation (Larese Filon et al., 2015; Poland et al., 2013). A recent review from Gimeno-Benito et al. (2021) (Gimeno-Benito et al., 2021) proposed the derivation of a worst-case potential dermal penetration value for NPs in their particulate form of 1% of the applied dose in intact skin, based on the compilation of 57 studies. However, more quantitative data and in particular studies based on the use of ex vivo studies on human or porcine skin are needed to assess the dermal absorption of NPs (Marquart et al., 2020). Several factors can affect the dermal absorption of NPs, such as the condition of the skin itself, i.e. the integrity of the skin (healthy or damaged) or the hydration of the skin, as well as the properties of the NPs, notably the formulation and physicochemical properties. In particular, size and surface chemistry appear to be critical factors in the dermal absorption of NPs (Poland et al., 2013).

Beyond the assessment of dermal exposure, decontamination of the skin after accidental exposure to NPs is also important to avoid any risk of systemic exposure, as well as any subsequent ingestion. However, there is currently no specific decontamination procedure for ENMs, and the effectiveness of skin decontamination protocols has been little studied to date (Magnano et al., 2021). In the present study, we focused on insoluble metallic NPs, titanium dioxide (TiO<sub>2</sub>), as these NPs are produced in large amounts, with an estimated 10,000 t produced each year worldwide (Piccinno et al., 2012), and are commonly used in personal care products or cosmetics, for example (Nohynek and Dufour, 2012). The skin permeation of TiO<sub>2</sub> NPs has been extensively studied, particularly due to its widespread use in sunscreens. However, a limited number of studies have reported that TiO<sub>2</sub> NPs can penetrate compromised skin down to the viable layers of the epidermis after sunscreen application to sunburnt skin in humans (Næss et al., 2016) or reach the dermis of healthy skin in minipigs (Sadrieh et al., 2010). Although TiO<sub>2</sub> NPs are considered safe for use in cosmetics because no evidence of carcinogenicity, mutagenicity or reproductive toxicity has been reported following dermal exposure (Dréno et al., 2019), in vitro studies have shown that TiO<sub>2</sub> NPs can induce the formation of reactive oxygen species (Rancan et al., 2014; Yin et al., 2012) and cytotoxicity in human keratinocytes (Crosera et al., 2015; Zhang et al., 2015). In the present study, we first assessed the diffusion kinetics of a commercial suspension of TiO<sub>2</sub> through the skin, using an ex vivo Franz diffusion cell as recommended (Marquart et al., 2020). We then compared the efficiency of three decontamination agents, water, liquid soap and a calixarene-based emulsion, in removing TiO<sub>2</sub> NPs from the skin. The experiments were conducted using a porcine ear skin model, a validated surrogate for human skin, widely used in permeation studies due to its characteristics close to those of human skin (Silva et al., 2022). Qualitative imaging techniques such as secondary ion mass spectrometry (SIMS) and quantitative techniques (inductively coupled plasma – mass spectrometry (ICP-MS) and single particle ICP-MS) were combined to quantify Ti ions and confirm the presence of NPs through the skin.

## 2. Materials and methods

### 2.1. Chemicals

PBS, pH 7.4 and nitric acid (HNO<sub>3</sub>) 69%, sulfuric acid (H<sub>2</sub>SO<sub>4</sub>) 97% and ammonium fluoride (NH<sub>4</sub>F) (>98%) were purchased from VWR (Rosny-sous-Bois, France). TiO<sub>2</sub> NPs (anatase/rutile) 40% in H<sub>2</sub>O (w/w), size <150 nm were purchased from Sigma-Aldrich while standard ionic Ti(IV) solution 1000 mg/L in 5% HNO<sub>3</sub>/0.5% HF was from VWR International. Trait rouge® cleaning gel was purchased from Sorifa

(Ostwald, France). Cevidra® decontamination emulsion containing 0.75% carboxylic calixarene was purchased from Cevidra laboratories (Grasse, France). D-squame® tape discs (Monaderm, Monaco, France) were used to generate excoriated skin.

### 2.2. Dispersion protocol

Commercial suspensions of TiO<sub>2</sub> NPs were sonicated for 1 min using an ultrasonic bath before being diluted in water to a concentration of 20 mg/L.

### 2.3. Characterization of TiO<sub>2</sub> NPs

#### 2.3.1. Transmission electron microscopy (TEM)

TEM analysis was carried out using a FEI/Tecnaï OSIRIS microscope operating at 200 kV. A few drops of TiO<sub>2</sub> suspension were deposited on a nickel grid coated with lacey carbon films, dried at room temperature, and placed in a vacuum chamber until analysis.

#### 2.3.2. Dynamic light scattering (DLS)

The hydrodynamic diameter of TiO<sub>2</sub> NPs was measured using a Zetasizer Nano ZS plus (Malvern Instruments). TiO<sub>2</sub> suspensions of 20 mg/L were prepared in water and sonicated for 1 min in an ultrasonic bath. 50 µL of suspension were analysed in triplicate in automatic mode. For each sample, the mean size was calculated using the Z-average of the three replicates.

#### 2.3.3. Single particle inductively coupled plasma mass spectrometry (Sp ICP-MS)

Sp ICP-MS analyses were carried out using a Nexion-2000 (Perkin-Elmer). The Sp ICP-MS operating parameters are summarized in Table 1. Mass spectrometry of titanium element can be performed either with the most abundant isotope <sup>48</sup>Ti or with <sup>47</sup>Ti. Here, the isotope <sup>48</sup>Ti was analysed in standard mode with a dwell time of 50 µs and a sampling time of 60 s. Particle and ionic calibration curves were prepared in water. Transport efficiency was assessed with the particle concentration-based method using a standard gold nanoparticle (50 nm Ultra Uniform Gold Nanospheres Nanocomposix) at 50000 part/mL. The ionic calibration curves ranged from 0 to 2 µg/L. The commercial suspension of TiO<sub>2</sub> NPs was diluted in water to a concentration of 0.5 µg/L and analysed using the Nano Application Module Syngistix software.

### 2.4. Preparation of the pigskin sample

The skin explants used for ex vivo transdermal diffusion of NPs or for skin decontamination studies were dissected from the outer surface of the ears of Landrace (female) or Piétrain (male) pigs. The pig ears were purchased from a slaughterhouse (Etablissements Harang, Houdan, France) after authorisation from the veterinary services (Direction Départementale des Services Vétérinaires des Hauts de Seine, France). No treatment or depilation using a blowtorch or hot water was carried out at the slaughterhouse prior to collection of the pig ears in order to preserve the integrity of the skin. The ears were gently cleaned in tepid

**Table 1**  
sp. ICP-MS operating parameters.

Parameters	
RF Power (Watts)	1500
Sample Flow rate (mL/min)	0.18
Analysis mode	Standard
Isotope monitored	<sup>48</sup> Ti
Dwell time (µs)	50
Total acquisition time (s)	60
TiO <sub>2</sub> density (g/cm <sup>3</sup> )	4.5
Ti mass fraction (%)	60
Transport efficiency (%)	9

water in the laboratory and stored at  $-20^{\circ}\text{C}$  until use. They were warmed to room temperature before each experiment, then full thickness pieces of skin were removed from the cartilage and prepared to fit the Franz diffusion cells. In accordance with OECD guidelines (OECD, 2004), only skin explants with a thickness  $<1$  mm, measured using a micrometric gauge (Mitutoyo, Roissy, France) were used. The excoriated skin used as a model of damaged or compromised skin (positive control allowing permeation of soluble ions and particles), was obtained by removing the stratum corneum of the epidermis by tape stripping using 60 adhesive tape discs (D-squame®, Monaderm, Monaco) per skin explant, as described previously (Spagnul et al., 2011).

## 2.5. Franz cell diffusion system and experimental set-up

Transcutaneous diffusion was carried out in accordance with the OECD guideline (OECD, 2004), as described previously (Spagnul et al., 2011). The experimental set-up is shown in Fig. 1.

Ex vivo transdermal diffusion studies of NPs through  $1.76\text{ cm}^2$  surfaces or skin decontamination were performed on six-Franz cell systems with automated sampling (MicroettePlus™, Teledyn-Hanson Research, Chatsworth, California, USA). The transepidermal water loss (TEWL) of each healthy or excoriated skin placed on the receptor compartment was measured before any diffusion test using a Tewameter TM 300® (Monaderm®, Monaco) equipped with an adapted probe to check the barrier function of the *stratum corneum*. According to the device's specifications, TEWL values below  $20\text{ g m}^{-2}\text{ h}^{-1}$  may reflect the integrity of the skin's barrier function ( $20 \pm 3\text{ g m}^{-2}\text{ h}^{-1}$  for healthy skin), while TEWL values above  $25\text{ g m}^{-2}\text{ h}^{-1}$  may indicate a breakdown in the skin's barrier function ( $27 \pm 1\text{ g m}^{-2}\text{ h}^{-1}$  for excoriated skin).

In the transdermal diffusion studies, we used PBS in the donor compartment for the Ti ions experiments to avoid the formation of a concentration gradient that would occur with differently charged fluids according to Fick's law of diffusion. In the case of  $\text{TiO}_2$  NPs experiments, as the commercial  $\text{TiO}_2$  suspension is formulated in aqueous phase, we diluted the NPs in water in order to reproduce a real exposure scenario. Thus, the skin in the donor compartments was exposed to a volume of  $600\text{ }\mu\text{L}$  of Ti ions at  $20\text{ mg/L}$  diluted in a PBS solution used as element control or to an aqueous suspension of  $\text{TiO}_2$  NPs. The corresponding dose of soluble titanium or  $\text{TiO}_2$  was  $12\text{ }\mu\text{g}$  ( $6.8\text{ }\mu\text{g/cm}^2$ ) and a total of 12 diffusion cells were used in each case. The receptor compartments were filled with a total volume of  $7\text{ mL}$  of PBS, homogenized by magnetic stirring ( $400\text{ rpm}$ ), and maintained at  $33.5^{\circ}\text{C}$  to ensure a skin surface temperature of  $32^{\circ}\text{C}$ . After skin exposure,  $1\text{ mL}$  aliquots of receptor fluid

were sampled at different times ( $0$ ;  $0.5$ ;  $6$ ;  $12$  and  $24\text{ h}$ ) to assess the diffusion kinetics of elemental Ti or  $\text{TiO}_2$  NPs.  $1\text{ mL}$  of fresh PBS was added to the receptor fluid after each sampling. The dilution factor of the receptor compartment between two subsequent samples was considered in calculating the percentage of Ti transferred. At the end of the  $24\text{-h}$  kinetics, the skins in the donor compartment were rinsed twice with  $1\text{ mL}$  of ultrapure water and then dried by applying, without rubbing, an absorbent tissue (Kimtech® paper). The skin explant and total receptor fluid were then collected and stored at  $-20^{\circ}\text{C}$  prior to Ti mass balance analysis.

## 2.6. Skin decontamination procedure

We evaluated the efficacy of two decontaminating agents, a classic liquid soap Trait rouge® (Sorifa), and a calixarene-based emulsion Cevibra® (Phan et al., 2013) to remove Ti contamination on healthy skin. Ultrapure water was used as a control (see Fig. 2).

In decontamination tests, a total of 12 skin biopsies were exposed to the same amount ( $12\text{ }\mu\text{g}$  or  $6.8\text{ }\mu\text{g/cm}^2$ ) and volume of  $\text{TiO}_2$  NPs. The decontamination products were added to the suspension either  $30\text{ min}$  (recommended time for early treatment) or  $6\text{ h}$  (representative of the end of a work shift) after contamination by the NPs ( $T_0$ ). Each treatment was first diluted to  $10\%$  with ultrapure water (formula/water  $1:10\text{ v/v}$ ) to simulate pre-wetting of the skin, before being added to the donor compartment in the same  $600\text{ }\mu\text{L}$  volume as for contamination. The mixture of treatment and contamination was left in contact for  $5\text{ min}$  before being removed by pipetting (using 3 back-and-forth movements of the pipette to simulate rinsing) for ICP-MS analysis. The skin surface was then rinsed twice with  $1\text{ mL}$  ultrapure water, and each skin explant was dried by applying, without rubbing, an absorbent tissue (Kimtech®). The skin explants were kept in the Franz diffusion system until  $T = 24\text{ h}$  after contamination, for comparison with the kinetic study. At the end of the  $24\text{ h}$ , the skin and the receptor fluid were recovered for the Ti mass balance.

Healthy skin explants were exposed ex vivo to  $\text{TiO}_2$  NP either for  $30\text{ min}$  to simulate early decontamination, or for  $6\text{ h}$  to represent a post-shift working day. The early treatment time of  $30\text{ min}$  was chosen because it is the usual average time required on work sites to transfer a victim to medical services and is recommended in French guidelines for skin decontamination (AFNOR, 2016).

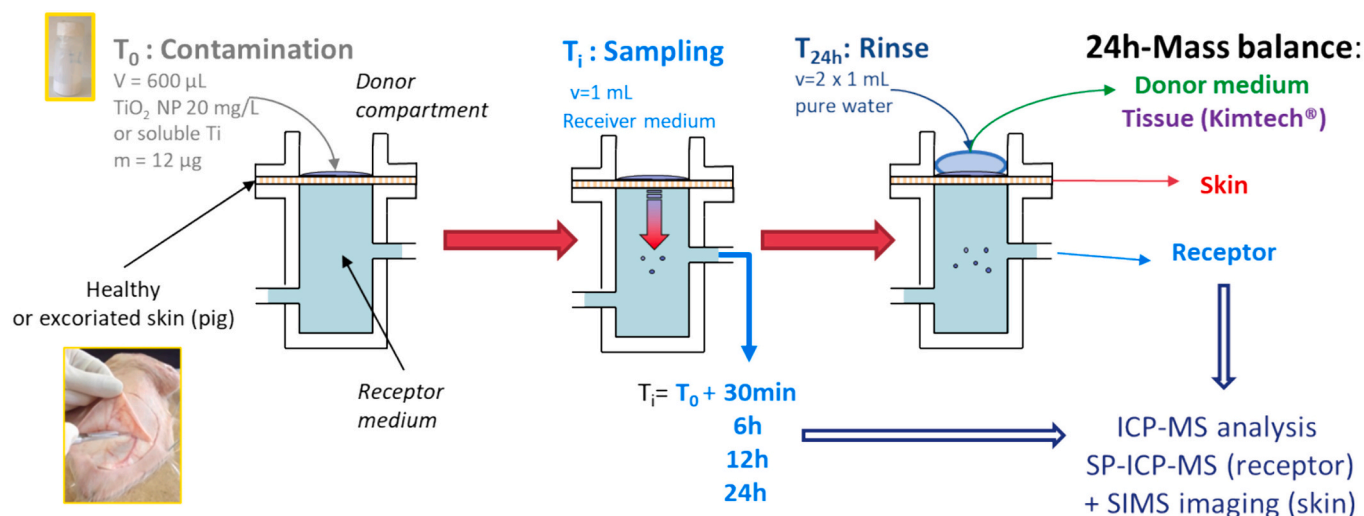


Fig. 1. Experimental set-up of skin diffusion studies. ICP-MS: inductively coupled plasma–mass spectrometry; SP-ICP-MS: single particle-inductively coupled plasma–mass spectrometry; SIMS: secondary ion mass spectrometry.

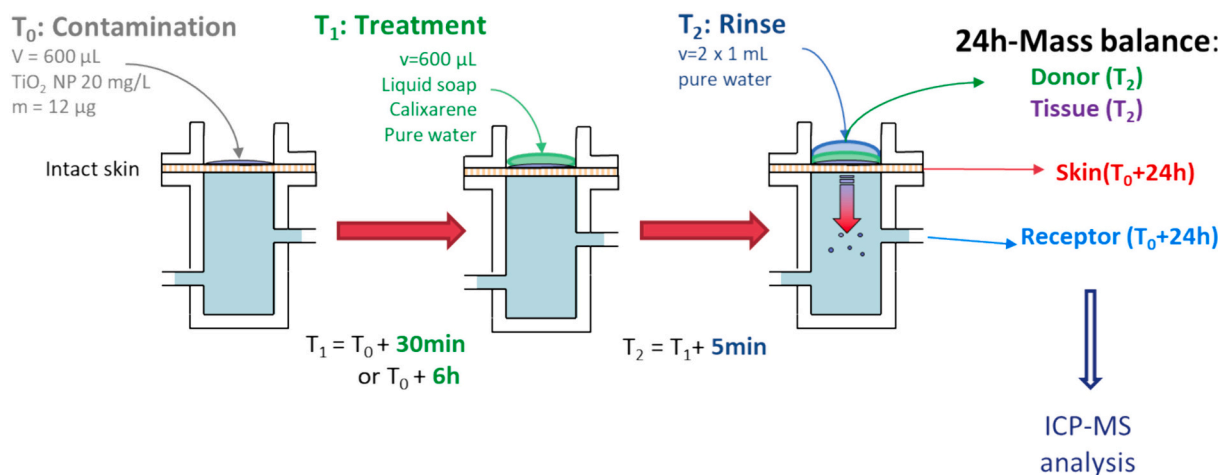


Fig. 2. Experimental set-up of skin decontamination studies. ICP-MS: inductively coupled plasma–mass spectrometry.

## 2.7. Analysis of Ti diffusion

### 2.7.1. Kinetics of Ti ions permeation in the receptor fluid

The iCAP-Q ICP-MS (Thermo Scientific) was used at IRSN to measure the level of Ti ions in the receptor fluid. The  $^{47}\text{Ti}$  isotope was analysed in standard mode with bismuth ( $^{209}\text{Bi}$ ) as an internal standard. The concentrations of the element Ti in the samples were determined using an external calibration curve comprising a set of 5 standards solutions with concentrations ranging from 0 to 10  $\mu\text{g/L}$  of Ti, obtained using a certified Ti solution.

The analytical detection (LOD) and quantification limits (LOQ) were 0.9 and 1.6  $\mu\text{g/L}$ , respectively.

### 2.7.2. Kinetics of permeation of $\text{TiO}_2$ NPs into the receptor fluid

The diffusion kinetics of Ti in the receptor fluid were measured using ICP-MS. The receptor fluids were mineralised prior to analysis at CEA in a 6% sulfuric acid solution and digested for 30 min in a microwave oven system (Anton Paar MW 3000) operating at 1100 W. The suspensions were then diluted 1:50 in 1%  $\text{HNO}_3$  and the  $^{47}\text{Ti}$  isotope was analysed using a Nexion 2000 (Perkin Elmer) operating in KED mode with helium at 2.2 mL/min.

External calibration curves including a set of 5 standard solutions with concentrations ranging between 0 and 25  $\mu\text{g/L}$  Ti were obtained using a certified ionic Ti solution. Yttrium ( $^{89}\text{Y}$ ) was added as an external standard. Two quality control standards (5 and 15  $\mu\text{g/L}$  Ti) were included to verify the accuracy of the calibration. The analytical LOD and LOQ were 14  $\mu\text{g/L}$  and 56  $\mu\text{g/L}$  of receptor fluid, respectively.

### 2.7.3. Ti mass balance after 24-h exposure to $\text{TiO}_2$ NPs

Ti levels at 24 h were measured in the donor compartment, the receptor fluid, the skin as well as the Kimtech® tissues. Samples were digested at IRSN in a mixture of  $\text{HNO}_3$  69% and 4.5 M ammonium fluoride (10:5 v/v) using the Ethos One® microwave oven system (Milestone) operating at 200 °C and 1000 W for 30 min. Digested samples were then diluted in 1%  $\text{HNO}_3$  for ICP-MS analysis.

ICP-MS analyses were performed using an iCAP-Q (Thermo Scientific).  $^{47}\text{Ti}$  isotope was analysed in standard mode using Bismuth ( $^{209}\text{Bi}$ ) as an internal standard. The concentrations of the element Ti in the samples were determined using an external calibration curve.

The analytical LOD and LOQ were 2.3 and 2.6  $\mu\text{g/L}$  respectively.

### 2.7.4. Sp ICP MS analysis of the receptor fluid

Analyses were performed using the parameters described above (see Table 1) with minor modifications. Both particle and ion calibration curves were prepared in 1:20 PBS and 0.1%  $\text{HNO}_3$ . Ionic calibration curves ranged from 0 to 2  $\mu\text{g/L}$ . Samples were diluted 1:20 in 0.1%

$\text{HNO}_3$ .

## 2.8. Localisation of $\text{TiO}_2$ in the skin

Samples of approximately 1  $\text{mm}^3$  were taken from skin explants exposed to  $\text{TiO}_2$  NPs for 24 h and fixed in a 2.5% glutaraldehyde bath buffered with sodium cacodylate for one day at 4 °C (conventional chemical fixation method used for tissue preservation (Suhard et al., 2018)). They were then dehydrated in successive ethanol and acetone baths and impregnated with epoxy resin. The resin was then polymerized for 48 h at 60 °C. *ultra-fine* serial sections 1  $\mu\text{m}$  deep were prepared by ultramicrotomy and deposited on polished silicon support for secondary ion mass spectrometry, or on a glass slide for histological control by photonic microscopy. SIMS imaging was carried out using an IMS 4F E7 SIMS and a NanoSIMS instrument (Cameca, Gennevilliers, France). For each of the areas analysed, images of ions with masses of 40 (calcium) and 23 (sodium) were selected to define the histological structure of the sample. The micro-localization of titanium in the skin layers was obtained by superimposing the  $^{48}\text{Ti}$  and  $^{23}\text{Na}$  images. Images were captured over areas of (500 × 500)  $\mu\text{m}^2$  or (250 × 250)  $\mu\text{m}^2$  with a primary beam intensity of 5 nA (IMS 4F E7) and over areas of (40 × 40)  $\mu\text{m}^2$  with a primary beam intensity of 20 pA. Under these analytical conditions, the lateral resolution of images was about 1.5  $\mu\text{m}$  and about 300 nm with IMS 4F E7 SIMS and NanoSIMS, respectively. Special attention was paid to the possible artefact induced by ultramicrotomy cutting. The absence of linear accumulation of  $\text{TiO}_2$  NPs at the edges of the ultra-thin section confirms that the cutting operation does not transport particles.

## 2.9. Statistical analysis

To compare the efficacy of the decontaminating products and treatment times, the variances of the series of data were analysed using the Fisher test. The means of the measurements were then compared using Student's *t*-test. Differences were considered significant when the *p*-value was less than the risk  $\alpha = 0.05$ .

## 3. Results

### 3.1. Characterization of $\text{TiO}_2$ NPs

TEM imaging showed irregularly shaped  $\text{TiO}_2$  NPs, which tended to form large agglomerates (Fig. 3). The average primary size was  $28 \pm 11$  nm, in line with the manufacturer's data, while the hydrodynamic diameter was  $167 \pm 3$  using DLS, compared with  $64 \pm 3$  nm using sp. ICP-MS (Table 2). The zeta potential was negative, close to  $-50$  mV

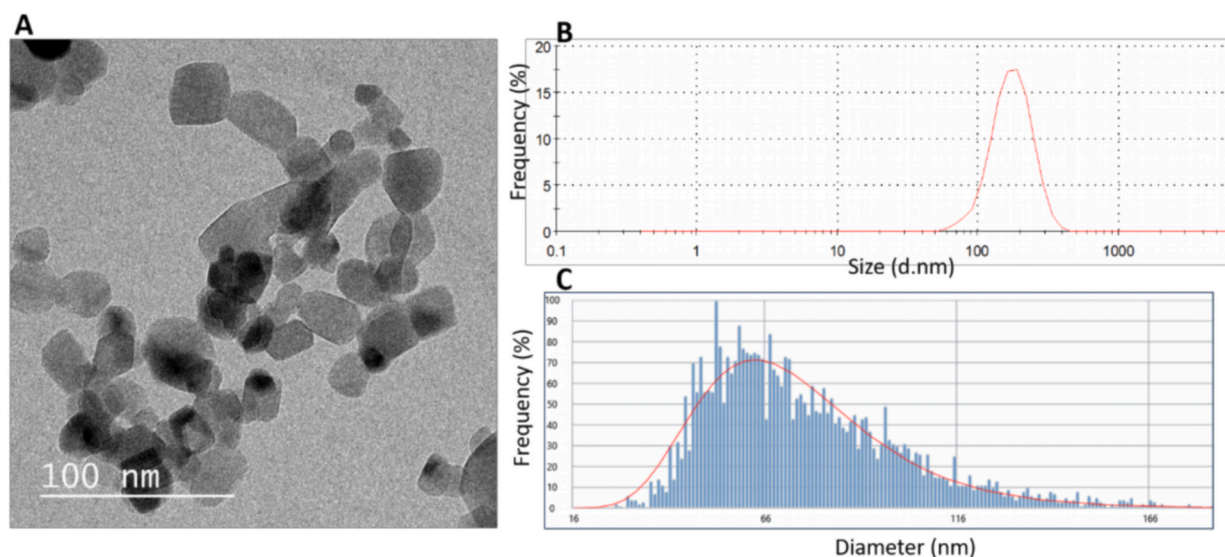


**Fig. 3.** TEM images (A), DLS diameter size-distribution (B) and sp. ICP-MS size-distribution histogram (C) of the commercial suspension of TiO<sub>2</sub> NPs in water.

**Table 2**

Physicochemical characteristics of the TiO<sub>2</sub>-NP suspension. Parameters are expressed as follow: mean value  $\pm$  standard deviation.

Parameters	TiO <sub>2</sub> in water	TiO <sub>2</sub> in PBS
Crystalline phase	Mixture of rutile and anatase	
Mean primary size by TEM - (nm) [Min-Max] (n = 100)	27.9 $\pm$ 10.7 [11–67]	ND
Mean hydrodynamic diameter by Z-average DLS - (nm) from 3 independent experiments	167.0 $\pm$ 3.1	669.5 $\pm$ 65.3
Mean Pdl	0.2	
Mean hydrodynamic diameter by sp. ICP-MS - (nm) from 3 independent experiments	64.4 $\pm$ 2.9	73.9 $\pm$ 0.3
Zeta potential (mV) (n = 3)	-49.7 $\pm$ 1	ND

ND: not determined.

Pdl: polydispersity index.

indicating that the suspension was very stable.

### 3.2. Percutaneous diffusion kinetics of Ti

#### 3.2.1. Kinetics of the permeation of TiO<sub>2</sub> NPs into the receptor fluid

The percutaneous diffusion of Ti into the receptor fluid was monitored in healthy or excoriated skin during 24 h of exposure to Ti ions or TiO<sub>2</sub> NPs. Excoriated skin exposed to Ti ions for 24 h served as a positive control. Ti accumulated in the receptor fluid as a function of time in excoriated skin exposed to Ti ions (Fig. S1 supplementary material) but not in the receptor fluid of healthy skin (Ti level < LOD). Regarding TiO<sub>2</sub> NPs, the levels of Ti were below our limit of detection at all sampling times, meaning that <0.1% of the applied dose of TiO<sub>2</sub> was able to permeate through both skin types under our experimental conditions.

Using sp. ICP-MS, TiO<sub>2</sub> NPs could be detected in some of the receptor fluids of both healthy and excoriated skin compared with the control after a 24 h exposure to TiO<sub>2</sub> NPs. However, we did not observe a higher permeation of TiO<sub>2</sub> NPs through excoriated skins compared to healthy skins, although it was not possible to reliably assess the concentration and size of these particles due to an insufficient number of peaks in the samples (see Fig. S2 in supplementary material).

#### 3.2.2. Ti mass balance after 24-h exposure to TiO<sub>2</sub> NPs

The total quantities of Ti measured in the different compartments of healthy skins after 24-h exposure to TiO<sub>2</sub> NPs are summarized in Table 3. A significant quantity of Ti (6%) was retained in the skin, while

**Table 3**

Mass balance of Ti in the different compartments of healthy skin after 24-h exposure to TiO<sub>2</sub> NPs. Results are expressed as a % of the applied dose (n = 12).

Compartment	Quantity of TiO <sub>2</sub> NP as a % of the applied dose (mean $\pm$ SD)
Donor	50 $\pm$ 8
Tissue	10 $\pm$ 5
Skin	6 $\pm$ 4
Receptor	0.1 $\pm$ 0.1
Total recovery	66 $\pm$ 17

the low diffusion of Ti through the skin, <0.1%, was confirmed. Most of the Ti was found mainly above the skin, in the donor compartment (50%) and on the surface of the skin (10% retrieved from tissues).

#### 3.2.3. TiO<sub>2</sub> imaging

The presence of particulate TiO<sub>2</sub> in healthy skin was assessed using SIMS imaging (Fig. 4). High-resolution SIMS imaging (nano-SIMS images) highlighted the presence of titanium in the stratum corneum and deeper in the epidermis (Fig. 4e). Small agglomerates of Ti-based NP (apparent size around 400 to 600 nm) were dispersed in the stratum corneum. Although the Ti intensities were low, the Ti also appeared to be homogeneously distributed in the epidermis at a lower content (Fig. 4g).

Complementary wide-field SIMS images – (200  $\times$  200)  $\mu\text{m}^2$  – indicate the presence of larger Ti-based NP agglomerates, ranging in size from 5 to 15  $\mu\text{m}$ . These agglomerates were found in the epidermis and around hair follicles. No agglomerates were detected in the control skin (Fig. 5).

### 3.3. Efficacy of skin decontamination treatments after exposure to TiO<sub>2</sub> NPs

The efficacy of soapy water and calixarene cleaning emulsion in removing Ti from the surface of healthy skin was compared to the efficacy of ultrapure water: the analysis of the mass balance of the compartments 24 h after skin exposure and decontamination 30 min or 6 h after exposure is presented in Table 4.

Delaying the decontamination process from 30 min to 6 h significantly increased Ti skin retention in water-treated skins and increased the diffusion of Ti into the receptor fluids in both water- and soap-treated skins. However, the use of a decontamination agent instead of water after a 6-h exposure resulted in a significant higher Ti retention in

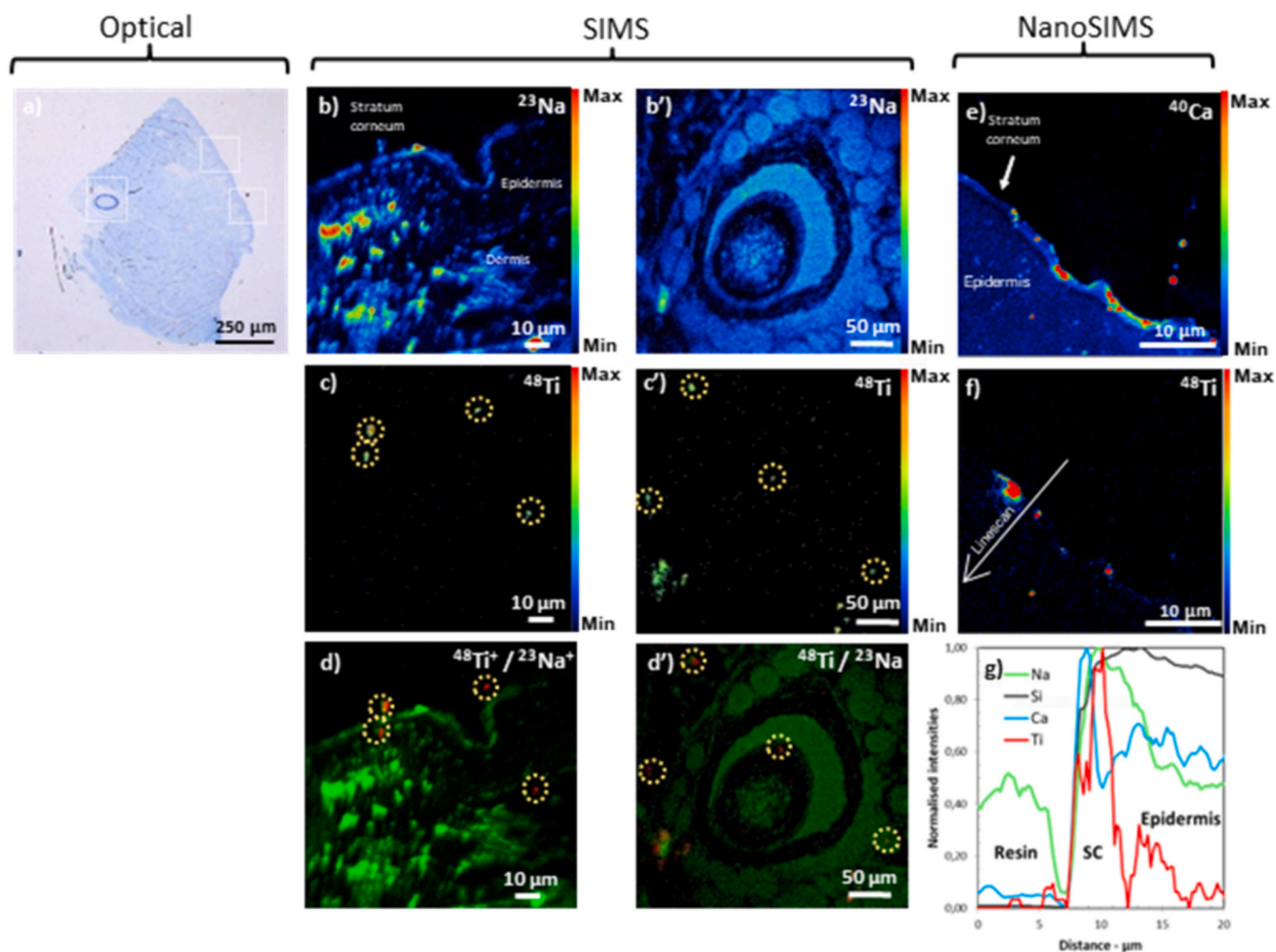


**Fig. 4.** (a) Histological view of hair follicle in a skin sample (3 area analysed). (b)(b') SIMS mapping of  $^{23}\text{Na}$ , (c)(c')  $^{48}\text{Ti}$ , (d)(d') overlay of  $^{48}\text{Ti}$  (red) on  $^{23}\text{Na}$  (green), (e) nanoSIMS mapping of  $^{40}\text{Ca}$  and (f)  $^{48}\text{Ti}$ , (g) evolution of Na, Si, Ca and Ti nanoSIMS intensities from the resin to the epidermis via the stratum corneum. (For interpretation of the references to colour in this figure legend, the reader is referred to the web version of this article.)

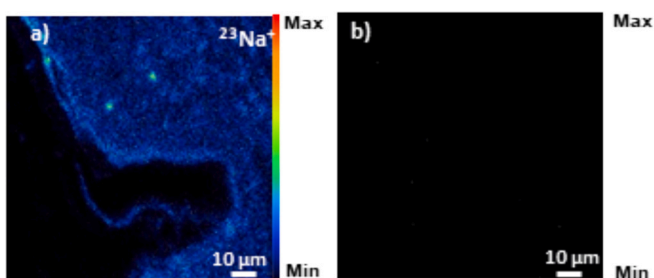


**Fig. 5.** SIMS mapping of the control skin. (a)  $^{23}\text{Na}$ , (b)  $^{48}\text{Ti}$

the donor compartment. Although calixarene was significantly more effective than water in reducing Ti levels in the skin after 6 h, the two decontamination agents generally showed comparable efficacy regardless of the time of treatment.

#### 4. Discussion

Our study showed that  $\text{TiO}_2$  NP could diffuse through both damaged and healthy skin, in small quantities, after exposure. With the aim of reproducing unintentional occupational exposure, a realistic dose of 20 mg/L of raw  $\text{TiO}_2$  suspension was tested. Exposure of excoriated skin to

**Table 4**

Ti mass balance in the different compartments of healthy skins at T = 24 h, after decontamination 30 min or 6 h after exposure to  $\text{TiO}_2$ . Results are expressed as a % of the applied dose (n = 12): mean value ± standard deviation.

Decontaminant agent	Water		Soap		Calixarene	
	30 min	6 h	30 min	6 h	30 min	6 h
Donor	75 ± 34	55 ± 6	101 ± 28	99 ± 23 <sup>b</sup>	114 ± 4 <sup>b</sup>	89 ± 6 <sup>b</sup>
Tissue	0.8 ± 0.5	17 ± 4 <sup>a</sup>	0.00 ± 0.1 <sup>b</sup>	12 ± 5 <sup>a</sup>	0.6 ± 0.3 <sup>c</sup>	5 ± 2 <sup>a, b, c</sup>
Skin	5 ± 6	12 ± 4 <sup>a</sup>	2 ± 3	7 ± 5	1 ± 2	5 ± 6 <sup>b</sup>
Receptor fluid	0.01 ± 0.1	0.2 ± 0.1 <sup>a</sup>	0.005 ± 0.008 <sup>a</sup>	0.09 ± 0.03 <sup>a</sup>	0.13 ± 0.05	0.12 ± 0.02
Total recovery	82 ± 41	84 ± 14	103 ± 31	118 ± 33	116 ± 6	99 ± 17

Significantly different values (p < 0.05).

<sup>a</sup> 30 min vs 6 h exposure.

<sup>b</sup> decontaminating agent vs water.

<sup>c</sup> soap vs calixarene.

soluble Ti ions showed a clear time-dependent accumulation in the

receptor fluid, confirming the validity of our experimental model and analytical method. The present findings confirm that  $<0.1\%$  of the applied dose of  $\text{TiO}_2$  can penetrate the pig skin model, which corresponds to the worst-case dermal penetration value estimated by Gimeno-Benito (Gimeno-Benito et al., 2021). The majority of applied  $\text{TiO}_2$  NPs (60%) remained on the surface of healthy skin after 24 h. Surprisingly, the total recovery of Ti in healthy skin after 24 h exposure to  $\text{TiO}_2$  was only  $66 \pm 17\%$ .  $\text{TiO}_2$  NPs and other types of NPs suspended in water are known to adsorb to plastic surfaces (Rozman et al., 2023). Despite the care taken to recover donor and receptor media by pipetting with plastic pipettes, loss of volume and possible adsorption of NPs to plastic materials or glass components may explain the variability of results from one diffusion cell to another and the loss of Ti in the mass balance. Sp ICP MS analyses confirmed the presence of low levels of  $\text{TiO}_2$  NPs in some of the receptor fluid samples, although it was not possible to reliably measure the size and the concentration of the NPs. This is because the presence of  $\text{Na}^+ \text{Cl}^-$  ions in the PBS solution used as the receptor fluid necessitated further dilution of the samples to reduce non-spectral interference, which is likely to reduce the sensitivity of the analysis (Loula et al., 2019). However, we did not observe a higher number of  $\text{TiO}_2$  NPs in the receptor fluids from excoriated ex vivo skin explants compared to healthy explants. We can assume that despite the loss of the most superficial layers of the epidermis, the NPs may still be retained in the deeper layers of the epidermis or the dermis. On the other hand, this study demonstrated a greater accumulation of  $\text{TiO}_2$  NPs in healthy skin compared with previous ex vivo studies. In particular, a systemically available dose of  $\text{TiO}_2$  (epidermis, dermis and receptor fluid) of  $<0.081 \pm 0.071\%$  and  $0.048 \pm 0.030\%$  (European Commission Directorate-General for Health and Food Safety, 2017) was reported in dermatomed pig skin exposed to  $760 \mu\text{g}/\text{cm}^2$  and  $816 \mu\text{g}/\text{cm}^2$  titanium in UV-filters, respectively, compared with  $6 \pm 4\%$  in our study. Although we did not quantify the amount of  $\text{TiO}_2$  in each skin compartment, the presence of Ti in SIMS images confirmed the potential penetration of particulate Ti into healthy skin after 24 h exposure. Our SIMS imaging indicates that Ti accumulation was not limited to the SC, as clusters of titanium were visualised in the epidermis, the dermis and around hair follicles.

It should be noted that most published data concern  $\text{TiO}_2$  NP present in sunscreens, with specific physicochemical properties compared to the raw suspension of  $\text{TiO}_2$  NPs tested here, despite comparable particle shapes and primary sizes (anatase/rutile with a diameter ranging from 20 to 50 nm) (Gontier et al., 2008; Janin et al., 2023; Peira et al., 2014). In particular, as the  $\text{TiO}_2$  NPs in sunscreens are rutile and formulated to remain on the surface of the skin, we expect that their reactivity and the extent of their penetration into the skin are different from those of our raw anatase/rutile NP suspension. Interestingly, anatase and anatase/rutile  $\text{TiO}_2$  NPs strongly disorganize the lipid bilayer in the SC compared to rutile  $\text{TiO}_2$  NPs which can result in increased skin permeability (Turci et al., 2013). On the other hand, the size and charge of the NPs can have an impact on their skin penetration. Smaller size is often associated with increased permeability, while the effect of the charge is more controversial (Poland et al., 2013). According to the manufacturer, the  $\text{TiO}_2$  NPs tested here were  $<150$  nm in diameter. While the primary size of the  $\text{TiO}_2$  NPs tested here was estimated at 30 nm using TEM, an over-estimated size by a factor of 2.6 was measured using DLS compared to sp. ICP-MS. The reason for this is that DLS reflects the hydrodynamic size which includes the solvation layer surrounding the NPs on the one hand, and on the other, DLS is sensitive to the presence of large particles, including agglomerates/aggregates, which scatter more light than smaller particles, thus increasing the mean diameter (Caputo et al., 2021; James and Driskell, 2013). Dermal permeation of the  $\text{TiO}_2$  NP suspension tested here occurred despite the presence of large aggregates as well as the strong electronegative charge that does not favour penetration through the negatively charged corneocytes of the SC, as demonstrated by Peira et al. (Peira et al., 2014). TEM images of the  $\text{TiO}_2$  NP suspension indicated the presence of small particles as well as large

aggregates. The smallest fraction of NPs can probably penetrate the skin while the larger fraction remains in the SC or cannot penetrate. In addition, our experiments were carried out in natural light, which allowed the  $\text{TiO}_2$  aggregates to disintegrate, resulting in increased permeation of  $\text{TiO}_2$  through the skin compared with dark conditions (Bennett et al., 2012). Finally, we cannot rule out that the penetration of  $\text{TiO}_2$  may be enhanced by the osmotic effect between the donor compartment containing water and the receptor compartment containing a PBS ionic solution necessary to maintain skin integrity throughout the experiment, and to mimic skin physiology, as recommended by the OECD (Guideline 428 and OECD guidance 28) (OECD, 2004). Besides, the permeation of  $\text{TiO}_2$  through the skin could also be altered in our ex vivo experimental conditions, as it is known that the diffusion of substances through frozen and thawed skins can be enhanced compared to fresh materials (Praça et al., 2018).

Although penetration and permeation of  $\text{TiO}_2$  following accidental exposure is low, effective skin decontamination is essential as it can lead to oral exposure. Decontamination traditionally consists of intensive washing with either water or soapy water, although the effectiveness of this process has been little studied (Magnano et al., 2021). In addition to water and soapy water, we tested the efficacy of calixarene emulsion, a cleansing emulsion consisting of an oil-in-water emulsion that proved effective in removing uranium compounds from the skin (Phan et al., 2013). In our experiments, effective decontamination was assessed by a higher retention of Ti in the donor compartment or in the tissue, as well as by a lower level of Ti in the skin or in the receptor fluid. In terms of total Ti mass balance, it is interesting to note that after application of products containing detergents (soapy water or calixarene emulsion), Ti recoveries were higher than after rinsing with pure water, probably due to a better desorption of NPs from inert surfaces or the epidermis of the skin. These observations are consistent with the NP adsorption hypothesis and the mechanism of action of decontamination products. After rinsing with water, our experiments show that, although the quantities measured in the receptor fluid remain negligible, a significant increase in Ti is observed in this compartment when the decontamination is delayed. This demonstrates the importance of treating the contamination quickly to limit Ti diffusion inside and through healthy skin. After contamination by  $\text{TiO}_2$  NPs, treatment with liquid soap, even if delayed for 6 h after skin exposure, retained significantly more Ti in the donor compartment ( $99 \pm 23\%$ ) than rinsing with water ( $55 \pm 6\%$ ) ( $p < 0.05$ ). Calixarene emulsion was also significantly more effective than water in retaining Ti in proportions  $>89\%$  in the donor compartment, independently of the treatment time ( $p < 0.05$ ). However, the efficacy of the two treatments, soapy water and calixarene emulsion, was comparable 30 min and 6 h after exposure of the skin to  $\text{TiO}_2$  NPs. This comparable efficacy could be attributed to the detergent effect of each treatment in eliminating the particulate forms of  $\text{TiO}_2$  deposited on the skin.

These results cannot be directly extrapolated to humans because the model can only demonstrate passive penetration through the epidermis and the appendages of healthy skin (sweat ducts, sweat glands and hair follicles) since we used non-viable skin explants without active processes such as phagocytosis, which has been described in keratinocytes in vitro (Lopes et al., 2016). Besides, the sweat-induced nanoparticle agglomeration of  $\text{TiO}_2$  described in vitro (Crosera et al., 2015; Li et al., 2022), could not be assessed under our ex vivo conditions. Nevertheless, this study draws attention to the importance of decontaminating the skin effectively and rapidly after exposure, as the epidermis can act as a reservoir for subsequent release of NPs into the dermis or even the systemic circulation.

## 5. Conclusion

Our experiments highlighted the possibility of a negligible permeation of  $\text{TiO}_2$  NPs through a model of healthy pig skin, following accidental exposure to a raw suspension of NPs, as well as low retention of Ti



in the layers of the skin. Decontamination using soapy water or calixarene emulsion effectively removed Ti from the skin surface. Our study highlighted the importance of decontaminating the skin as soon as possible after exposure in order to avoid the retention of TiO<sub>2</sub> NPs through the skin. As perspectives, the effectiveness of cleansing products could be evaluated on other crystalline forms of TiO<sub>2</sub> NPs (pure rutile or anatase). Future investigations will focus on skin decontamination following exposure to silver NPs, another type of NPs known to dissolve in biological media.

## Funding

This study was supported by the Anses National Environmental and Occupational Health Research Program (EST/ 2019/1/087).

## CRediT authorship contribution statement

**Adeline Tarantini:** Writing – review & editing, Writing – original draft, Methodology, Investigation, Formal analysis, Data curation. **Emilie Jamet-Anselme:** Methodology, Investigation. **Sabine Lam:** Methodology, Investigation. **Vincent Haute:** Methodology, Investigation. **David Suhard:** Methodology, Investigation. **Nathalie Valle:** Methodology, Investigation. **Véronique Chanel-Mossuz:** Project administration, Funding acquisition, Conceptualization. **Céline Bouvier-Capely:** Writing – review & editing, Project administration, Methodology, Funding acquisition, Data curation, Conceptualization. **Guillaume Phan:** Writing – review & editing, Writing – original draft, Methodology, Investigation, Conceptualization.

## Declaration of competing interest

The authors report there are no competing interests to declare.

## Data availability

The authors confirm that the data supporting the findings of this study are available in the article and its supplementary documents.

## Acknowledgment

The authors would like to thank François Saint-Antonin at the Nanocharacterization Platform of the CEA Grenoble for the TEM images, Esther Lentzen (LIST, Luxembourg) and Brahime El Adib (LIST, Luxembourg) for their contribution to nano-SIMS imaging.

## Appendix A. Supplementary data

Supplementary data to this article can be found online at <https://doi.org/10.1016/j.tiv.2024.105918>.

## References

- AFNOR, 2016. Security and Protection of Citizens - CBRN-E-Protocols for Performance Assessment of Technologies Intended for Undamaged Skin Decontamination.
- Bennett, S.W., Zhou, D., Mielke, R., Keller, A.A., 2012. Photoinduced disaggregation of TiO<sub>2</sub> nanoparticles enables transdermal penetration. *PLoS ONE* 7, e48719.
- Bergamaschi, E., 2009. Occupational exposure to nanomaterials: present knowledge and future development. *Nanotoxicology* 3, 194–201.
- Caputo, F., Vogel, R., Savage, J., Vella, G., Law, A., Della Camera, G., Hannon, G., Peacock, B., Mehn, D., Ponti, J., Geiss, O., Aubert, D., Prina-Mello, A., Calzolari, L., 2021. Measuring particle size distribution and mass concentration of nanoplastics and microplastics: addressing some analytical challenges in the sub-micron size range. *J. Colloid Interface Sci.* 588, 401–417.
- Crosera, M., Prodi, A., Mauro, M., Pelin, M., Florio, C., Bellomo, F., Adami, G., Apostoli, P., De Palma, G., Bovenzi, M., Campanini, M., Filon, F.L., 2015. Titanium dioxide nanoparticle penetration into the skin and effects on HaCaT cells. *Int. J. Environ. Res. Public Health* 12, 9282–9297.
- Dréno, B., Alexis, A., Chuberre, B., Marinovich, M., 2019. Safety of titanium dioxide nanoparticles in cosmetics. *J. Eur. Acad. Dermatol. Venereol.* 33, 34–46.
- European Commission Directorate-General for Health and Food Safety, 2017. Opinion on Titanium Dioxide (Nano Form) Coated with Cetyl Phosphate, Manganese Dioxide or Triethoxycaprylsilane as UV-Filter in Dermal Applied Cosmetic. Publications Office.
- Gimeno-Benito, I., Giusti, A., Dekkers, S., Haase, A., Janer, G., 2021. A review to support the derivation of a worst-case dermal penetration value for nanoparticles. *Regul. Toxicol. Pharmacol.* 119, 104836.
- Gontier, E., Ynsa, M.-D., Břřr, T., Hunyadi, J., Kiss, B., Gáspár, K., Pinheiro, T., Silva, J.-N., Filipe, P., Stachura, J., Dabros, W., Reinert, T., Butz, T., Moretto, P., Surlève-Bazeille, J.-E., 2008. Is there penetration of titania nanoparticles in sunscreens through skin? A comparative electron and ion microscopy study. *Nanotoxicology* 2, 218–231.
- James, A.E., Driskell, J.D., 2013. Monitoring gold nanoparticle conjugation and analysis of biomolecular binding with nanoparticle tracking analysis (NTA) and dynamic light scattering (DLS). *Analyst* 138, 1212–1218.
- Janin, M., Delaune, A., Gibouin, D., Delaroche, F., Klaes, B., Etienne, A., Cabin-Flaman, A., 2023. The high resolutive detection of TiO<sub>2</sub> nanoparticles in human corneocytes via TEM/NanoSIMS correlation. *Appl. Sci.* 13, 12189.
- Larese Filon, F., Mauro, M., Adami, G., Bovenzi, M., Crosera, M., 2015. Nanoparticles skin absorption: new aspects for a safety profile evaluation. *Regul. Toxicol. Pharmacol.* 72, 310–322.
- Lekki, J., Stachura, Z., Dąbroś, W., Stachura, J., Menzel, F., Reinert, T., Butz, T., Pallon, J., Gontier, E., Ynsa, M.D., Moretto, P., Kertesz, Z., Szikszai, Z., Kiss, A.Z., 2007. On the follicular pathway of percutaneous uptake of nanoparticles: ion microscopy and autoradiography studies. *Nucl. Instrum. Methods Phys. Res., Sect. B* 260, 174–177.
- Li, J., Dong, J., Huang, Y., Su, J., Xie, Y., Wu, Y., Tang, W., Li, Y., Huang, W., Chen, C., 2022. Aggregation kinetics of TiO<sub>2</sub> nanoparticles in human and artificial sweat solutions: effects of particle properties and sweat constituents. *Environ. Sci. Technol.* 56, 17153–17165.
- Lopes, V.R., Loitto, V., Audinot, J.N., Bayat, N., Gutleb, A.C., Cristobal, S., 2016. Dose-dependent autophagic effect of titanium dioxide nanoparticles in human HaCaT cells at non-cytotoxic levels. *J. Nanobiotechnol.* 14.
- Loula, M., Kaňa, A., Mestek, O., 2019. Non-spectral interferences in single-particle ICP-MS analysis: an underestimated phenomenon. *Talanta* 202, 565–571.
- Magnano, G.C., Rui, F., Larese Filon, F., 2021. Skin decontamination procedures against potential hazards substances exposure. *Chem. Biol. Interact.* 344, 109481.
- Malik, S., Muhammad, K., Waheed, Y., 2023. Nanotechnology: a revolution in modern industry. *Molecules* 28, 661.
- Marquart, H., Park, M., Giannakou, C., Vandebriel, R., Wijnhoven, S., Lazarska, K., 2020. A Critical Review of the Factors Determining Dermal Absorption of Nanomaterials and Available Tools for the Assessment of Dermal Absorption. European Chemicals Agency.
- Næss, E.M., Hofgaard, A., Skaug, V., Gulbrandsen, M., Danielsen, T.E., Grahnstedt, S., Skogstad, A., Holm, J.-Ø., 2016. Titanium dioxide nanoparticles in sunscreen penetrate the skin into viable layers of the epidermis: a clinical approach. *Photodermatol. Photoimmunol. Photomed.* 32, 48–51.
- Nohynek, G.J., Dufour, E.K., 2012. Nano-sized cosmetic formulations or solid nanoparticles in sunscreens: a risk to human health? *Arch. Toxicol.* 86, 1063–1075.
- OECD, 2004. OECD, Guideline for the Testing of Chemicals. Draft Guideline 428: Skin Absorption: (In Vitro Method).
- Peira, E., Turci, F., Corazzari, I., Chirio, D., Battaglia, L., Fubini, B., Gallarate, M., 2014. The influence of surface charge and photo-reactivity on skin-permeation enhancer property of nano-TiO<sub>2</sub> in ex vivo pig skin model under indoor light. *Int. J. Pharm.* 467, 90–99.
- Phan, G., Semili, N., Bouvier-Capely, C., Landon, G., Mekhloufi, G., Huang, N., Rebière, F., Agarande, M., Fattal, E., 2013. Calixarene cleansing formulation for uranium skin contamination. *Health Phys.* 105, 382–389.
- Piccinno, F., Gottschalk, F., Seeger, S., Nowack, B., 2012. Industrial production quantities and uses of ten engineered nanomaterials in Europe and the world. *J. Nanopart. Res.* 14, 1109.
- Poland, C.A., Read, S.A.K., Varet, J., Carse, G., Christensen, F.M., Hankin, S.M., 2013. Dermal absorption of nanomaterials - part of the “better control of nano”. In: Initiative 2012–2015. Environmental Project No. 1504, 2013. The Danish Environmental Protection Agency, Copenhagen.
- Praça, F.S.G., Medina, W.S.G., Eloy, J.O., Petrilli, R., Campos, P.M., Ascenso, A., Bentley, M.V.L.B., 2018. Evaluation of critical parameters for in vitro skin permeation and penetration studies using animal skin models. *Eur. J. Pharm. Sci.* 111, 121–132.
- Rancan, F., Nazemi, B., Rautenberg, S., Ryll, M., Hadam, S., Gao, Q., Hackbarth, S., Haag, S.F., Graf, C., Rühl, E., Blume-Peytavi, U., Lademann, J., Vogt, A., Meinke, M. C., 2014. Ultraviolet radiation and nanoparticle induced intracellular free radicals generation measured in human keratinocytes by electron paramagnetic resonance spectroscopy. *Skin Res. Technol.* 20, 182–193.
- Roco, M.C., 2011. The long view of nanotechnology development: The National Nanotechnology Initiative at 10 years. In: Roco, M.C., Hersam, M.C., Mirkin, C.A. (Eds.), *Nanotechnology Research Directions for Societal Needs in 2020: Retrospective and Outlook*. Springer, Netherlands, Dordrecht, pp. 1–28.
- Rozman, U., Klun, B., Marolt, G., Imperl, J., Kalčíková, G., 2023. A study of the adsorption of titanium dioxide and zinc oxide nanoparticles on polyethylene microplastics and their desorption in aquatic media. *Sci. Total Environ.* 888, 164163.
- Sadrieh, N., Wokovich, A.M., Gopee, N.V., Zheng, J., Haines, D., Parmiter, D., Siitonen, P.H., Cozart, C.R., Patri, A.K., McNeil, S.E., Howard, P.C., Doub, W.H., Buhse, L.F., 2010. Lack of significant dermal penetration of titanium dioxide from sunscreen formulations containing nano- and submicron-size TiO<sub>2</sub> particles. *Toxicol. Sci.* 115, 156–166.

- Schulte, P., Geraci, C., Zumwalde, R., Hoover, M., Castranova, V., Kuempel, E., Murashov, V., Vainio, H., Savolainen, K., 2008. Sharpening the focus on occupational safety and health in nanotechnology. *Scand. J. Work Environ. Health* 471–478.
- Silva, I.R., Lima, F.A., Reis, E.C.O., Ferreira, L.A.M., Goulart, G.A.C., 2022. Stepwise protocols for preparation and use of porcine ear skin for in vitro skin permeation studies using Franz diffusion cells. *Curr. Protoc.* 2.
- Spagnul, A., Bouvier-Capely, C., Phan, G., Landon, G., Tessier, C., Suhard, D., Rebière, F., Agarande, M., Fattal, E., 2011. Ex vivo decrease in uranium diffusion through intact and excoriated pig ear skin by a calixarene nanoemulsion. *Eur. J. Pharm. Biopharm.* 79, 258–267.
- Suhard, D., Tessier, C., Manens, L., Rebière, F., Tack, K., Agarande, M., Guéguen, Y., 2018. Intracellular uranium distribution: comparison of cryogenic fixation versus chemical fixation methods for SIMS analysis. *Microsc. Res. Tech.* 81, 855–864.
- Turci, F., Peira, E., Corazzari, L., Fenoglio, I., Trotta, M., Fubini, B., 2013. Crystalline phase modulates the potency of nanometric TiO<sub>2</sub> to adhere to and perturb the stratum corneum of porcine skin under indoor light. *Chem. Res. Toxicol.* 26, 1579–1590.
- Yin, J.-J., Liu, J., Ehrenshaft, M., Roberts, J.E., Fu, P.P., Mason, R.P., Zhao, B., 2012. Phototoxicity of nano titanium dioxides in HaCaT keratinocytes—generation of reactive oxygen species and cell damage. *Toxicol. Appl. Pharmacol.* 263, 81–88.
- Zhang, X., Li, W., Yang, Z., 2015. Toxicology of nanosized titanium dioxide: an update. *Arch. Toxicol.* 89, 2207–2217.